IJAREEIE

e-ISSN: 2278-8875
p-ISSN: 2320-3765

# International Journal of Advanced Research in Electrical, Electronics and Instrumentation Engineering

Volume 10, Issue 12, December 2021

INTERNATIONAL STANDARD SERIAL NUMBER INDIA

Impact Factor: 7.282

9940 572 462 | 6381 907 438 | ijareeie@gmail.com | www.ijareeie.com

| e-ISSN: 2278 – 8875, p-ISSN: 2320 – 3765| www.ijareeie.com | Impact Factor: 7.282|

|| Volume 10, Issue 12, December 2021 ||

DOI:10.15662/IJAREEIE.2021.1012029

# Harmonic Analysis of Off-Grid Solar System for Non-Linear Load

**Mitali Sisodiya[1], R.S. Mandloi[2]**

PG Student [P.E.], Dept. of EE, S.G.S.I.T.S., Indore, M.P., India[1]

Assistant Professor, S.G.S.I.T.S., Indore, M.P., India[2]

**ABSTRACT:** To obtain usable solar power with solar Photo Voltaic (SPV) deploys Power Electronic Converters (PEC) since output power from solar is DC and converters convert it into AC. PEC interfacing hinders the operation of utility system. The high frequency switching operation injects the harmonics into the system, due to this output wave form at PCC gets distorted, and various Power Quality (PQ) issues are generated. In this paper, performance analysis of off-grid Solar Energy Conversion System under with two-level Voltage Source Inverter (VSI) to reduce harmonics is presented. In this paper brief overview of Solar Energy Conversion System (SECS) is presented. Mathematical modeling of solar PV (SPV) system is described. For satisfactory performance of SECS, Maximum Power Point Tracking (MPPT) algorithm also play very important role. Brief overview of conventional MPPT algorithms is also given. The main Components of SECS is DC-DC converter and DC-AC inverter which is discussed in detail with control topologies. The scope of the proposed work is to present power quality improvement in off-grid SECS system. The performance of the system has been analyzing for various operating conditions of balanced unbalanced non-linear load.

**KEYWORDS:** Off-grid, PV system, SECS, Modeling, MATLAB/Simulink

## I.INTRODUCTION

Solar power is becoming one of the vast power generation systems all over the world. The sharp drop in prices of solar technologies by about 52% between 2010 and 2015 (in terms of kW) has changed the relative importance of solar energy. Tropical countries, including India, are rich in the solar resource, and can use this in an innovative way to meet energy needs at decentralized locations. The Solar Energy Conversion System (SECS) is proving to be a promising future energy technology of RE projects. The SECS is a technology through which solar energy obtained from sun's radiation can be converted into useful electricity via various synthesizing stages of conversion. The synthesizing stages comprises of PV cell which is the elementary building block of SECS; PV panel, which is the series/parallel combination of PV module. MPPT which track the maximum output for the given input at any instant and DC/AC conversion controllers. While designing SECS the biggest challenge is to transform the stochastic behavior of PV sources into a system with ease of controllability [8]. This is assisted by the advance PEC technology.

Installation of solar PV panels to produce bulk power can be Stand Alone Mode (SAM) or Grid Connected Mode (GCM). The stand-alone (SA) system is installed to meet the local supply demand and to operate as application-oriented utility like pump storage system, street lighting, solar heater etc.SA-SECS is worthy in forming a microgrid which can be operated to meet the power demand of remote area where transmission is either infeasible or uneconomical. In Fig. 2., SECS will operate in SAM. In SAM, SECS comprises of PV-panel, DC-DC converter, DC-AC inverter, Filter, and load bus. The DC-Dc converter control is designed using MPPT and PI controller. The element of inverter control is PLL and PI controller for voltage and current regulation at load bus. Another way of harnessing solar power is to operated SECS in GCM. Now a day's grid connected PV systems are gaining more popularity as they do not need any storage device and offers optimum use of PV generated energy. Application in distributed generation is also another major advantage of GCM [2]. Grid connected PV system offers the advantage of feeding excess power generated into the grid. For efficient gird integration of SECS, several actions need to be taken to address various issues, such as flexible power generation with distributed as well as conventional sources, voltage/frequency control (V-FC), establishment of Renewable Energy Management Centers, etc., [3]. For large scale SECS integration, voltage regulation, power balancing and stability are the main control function of the model. Stability here talks about the ability of the system to retain stable operational limits with high SECS penetration to operate under contingency events like, faults, voltage transients, relay mal-operation, intermittent renewable energy sources behavior etc. In this work performance analysis of SA-SECS is presented.

| e-ISSN: 2278 – 8875, p-ISSN: 2320 – 3765| www.ijareeie.com | Impact Factor: 7.282|

|| Volume 10, Issue 12, December 2021 ||

DOI:10.15662/IJAREEIE.2021.1012029

## II. MATHEMATICAL MODELING OF PV ARRAY (PVA)

The elementary building block of PVA is PV cell, which is formed with p-n junction having thin wafer of semiconductor material. When light with energy greater than the energy band-gap ($E_g$) of the semiconductor falls it get absorbed and electron-hole pairs are formed resulting in the generation of DC output across terminals. In this work single diode module of PV cell with Ns series and $N_P$ parallel module is employed as represented in Fig 1.

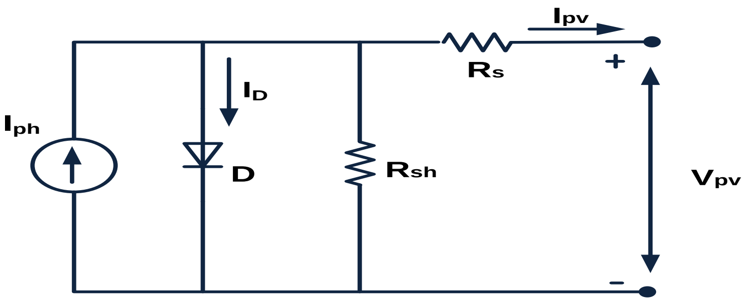


Fig.1 Simplified equivalent circuit of a PV cell

The PV cell behaves as an ideal current source generating photon current $I_{PH}$. When the law of current by (KCL) is applied in Fig. 1, the output current $I_{PV}$ can be represented as by eq. (1)

$$I_{PV} = I_{PH} - I_D \tag{1}$$

$$I_D = I_S\left[exp\left(\frac{q(V_{PV}+IR_S)}{N_S KAT_O}\right) - 1\right] \tag{2}$$

$$I_{PV} = I_{PH} - I_S\left[exp\left(\frac{q(V_{PV}+IR_S)}{N_S KAT_O}\right) - 1\right] \tag{3}$$

For a PV array having $N_P$ parallel module eq. (3) can be modified as;

$$I_{PV} = N_P * I_{PH} - N_P * I_S\left[exp\left(\frac{q(V_{PV}+IR_S)}{N_S KAT_O}\right) - 1\right] \tag{4}$$

$$V_{PV} = \left[\frac{N_S KAT_O}{q}\ln(1-(I_{PV} - N_P * I_{PH} + N_P * I_S) - 1\right] \tag{5}$$

Where $I_{PH}$ and $I_S$ are presented in eq. (6) and eq. (7) respectively,

$$I_{PH} = [I_{SC} + K_i(T_O - T_r)] * \frac{G}{G_{ref}} \tag{6}$$

$$I_S = I_{SC}\left[\frac{T_O}{T_r}\right]^3 exp\left[\left(\frac{qE_g}{AK}\right)\left(\frac{1}{T_r} - \frac{1}{T_O}\right)\right] \tag{7}$$

$I_D$=is the current across diode
$I_{ph}$= is the solar induced or photon generated current
$G_{ref}$ =is the reference irradiance 1000 W/m$^2$
$G$ =is the measured irradiance W/m$^2$
$I_s$ = diode saturation current
$V_{PV}$ =is the output voltage across terminal of solar cell
$k$ = Boltzmann constant
$K_i$= is the temperature coefficient of *Isc*
$T_O$ = solar cell operating temperature
$q$ = elementary electron charge
$A$ =diode quality factor (diode emission coefficient).
$I_{SC}$ = is the short circuit current of solar cell

| e-ISSN: 2278 – 8875, p-ISSN: 2320 – 3765| www.ijareeie.com | Impact Factor: 7.282|

|| Volume 10, Issue 12, December 2021 ||

DOI:10.15662/IJAREEIE.2021.1012029

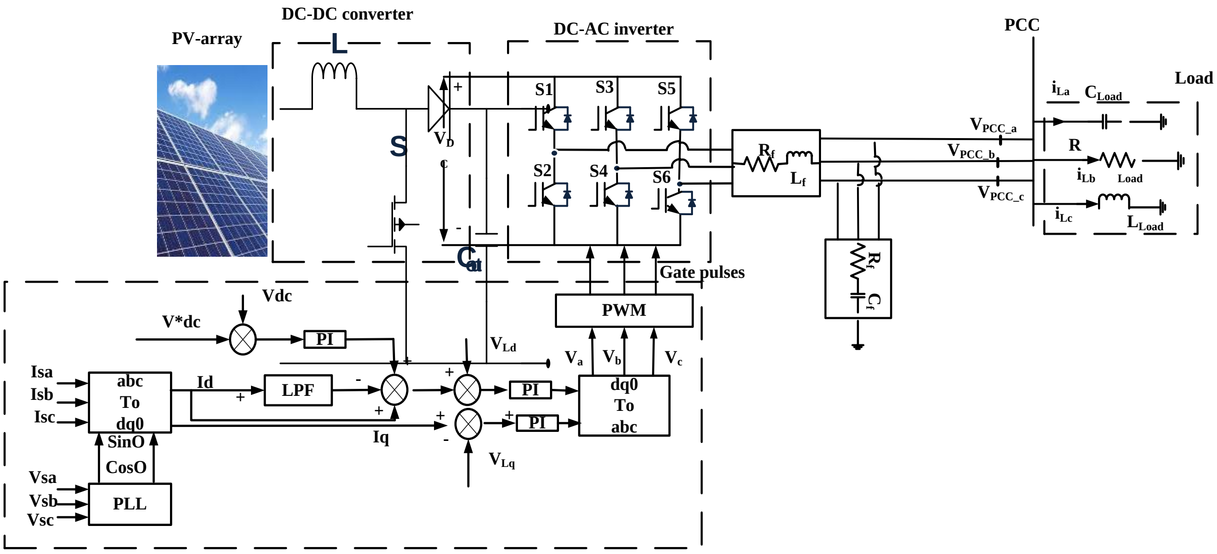


Fig. 2 The schematic diagram of proposed SECS

$R_S$ is the series resistance which a solar cell offers to the movement of electrons $R_{SH}$ depicts the losses associated with leakage current through a parallel resistive path within the device. The parameters of the module is given in Table 1.

Table 1. Paramaters for designing SECS system

| S No. | Parameter | Variable | Value |
|---|---|---|---|
| 1 | Maximum PV power (STC) | Pmax | 25 KW |
| 2 | Maximum voltage at Pmax | Vmp | 65 V |
| 3 | Maximum current at Pmax | Imp | 6 A |
| 4 | Open-circuit voltage | Voc | 46.22 V |
| 5 | Short-circuit current | Isc | 9.06 A |
| 6 | Series cells | $N_S$ | 10 |
| 7 | Parallel cells | $N_P$ | 10 |
| 8 | Ideality factor of diode | A | 1.3 |
| 9 | Cell short circuit current temperature coefficient of Isc | Ki | 0.058 ◦C |
| 10 | Reference-temperature | Tref | 25 ◦C |
| 11 | Irradiance | Gref | 1000 at STC |

**Maximum Power Point Tracking (MPPT)**

P&O method is commonly used method because its implementation circuitry is not complex but it shows good response where environmental conditions changes rapidly. Hill climbing is also similar to P&O method but it involves perturbation in duty cycle. It is simple to implement but its tracking speed is slow. RCC method takes the advantage of the signal ripple, which is automatically present in power converters. RCC is a complex process hence accuracy is low. In soft computing techniques like PSO, ANN and fuzzy logic has high efficiency but not cost effective. The Inc. Con. Method has good tracking efficiency, but its circuit is complex.In the proposed work, P&O Method of MPPT is employed to track the maximum power operating point due to its ease to control and good tracking characteristics. The method is basically iterative approach, in which operating point of solar PV oscillates around the maximum power point. The power versus voltage curve of solar PV shows that, change in power with respect to voltage *(dP/dV)* is positive, negative and zero for region before maximum power point, after maximum power point and at maximum power point respectively. This method is applied by perturbing the operating voltage at regular interval and oscillating around the point *dP/dV=0* i.e. MPP. The operation explained in Table 2.1.

| e-ISSN: 2278 – 8875, p-ISSN: 2320 – 3765| www.ijareeie.com | Impact Factor: 7.282|

|| Volume 10, Issue 12, December 2021 ||

DOI:10.15662/IJAREEIE.2021.1012029

Table 2. Methodology of P&O Method

| Perturbation | Change in power | Next perturbation |
|---|---|---|
| Positive | Positive | Positive |
| Positive | Negative | Negative |
| Negative | Positive | Negative |
| Negative | Negative | Positive |

## III. DC-DC CONVERTERS

### Boost converter

Boost converter increases the generated voltage as compared to low input voltage. The boost converter topology is shown in Fig. 3. When the switch $S_1$ is turned on by the pulse of PWM, current flows through the inductor (L) and energy are stored in it. When switch is turned off, energy stored in the inductor in the form of magnetic field provides an induced voltage across the inductor that adds to the input voltage. The input voltage and voltage across the inductor are in series and collectively charge the output capacitor ($C_{out}$) to a voltage higher than input voltage.

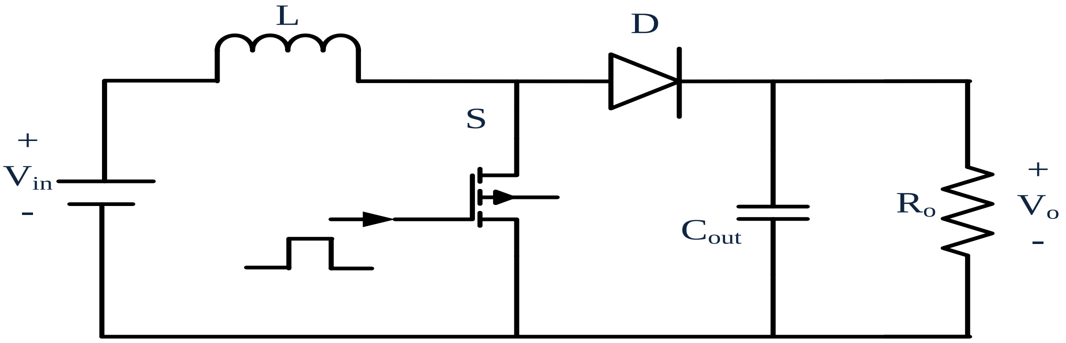


Fig. 3 Circuit diagram of boost converter

The values for D, switching frequency $f_s$, load current $I_o$, Ripple current $\Delta I_0$, Inductor L, Capacitor $C_{out}$, is presented in Table 3. with the design parameter of DC-DC converter. Fig. 6 shows the comparison of input voltage (Ppv) and the DC-DC converter output voltage at the output terminal. The $V_i$ is around 400 V and the $V_o$ is around 600 V.

Table 3. Design parameter of DC-DC converter

| S No. | Parameter | Expression | Value |
|---|---|---|---|
| 1 | Duty cycle (D) | $D = 1 - \left(\frac{V_i}{V_o}\right)$ | 70% |
| 2 | Switching frequency | $f_s$ | 5 KHz |
| 3 | Load current ($Io$) | $\frac{V_o}{R_0} = \frac{V_i}{R_0(1-D)}$ | 100 A |
| 4 | Ripple current ($\Delta I_0$) | $\Delta I_O = 0.1 \times I_O$ | 0.04 |
| 5 | Inductor ($L$) | $L = \frac{V_i \times D}{\Delta I_L \times f_s}$ | 0.99mH |
| 6 | Capacitor ($C_{out}$) | $C = \frac{D}{R_o \times f_s \times 0.01}$ | 1000µF |

| e-ISSN: 2278 – 8875, p-ISSN: 2320 – 3765| www.ijareeie.com | Impact Factor: 7.282|

|| Volume 10, Issue 12, December 2021 ||

DOI:10.15662/IJAREEIE.2021.1012029

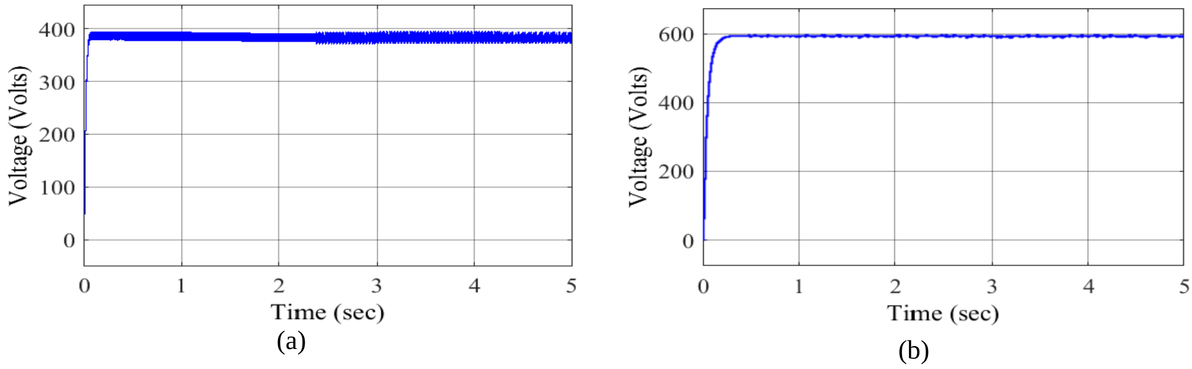


Fig. 4 Voltage waveforms of DC-DC converter: (a) input voltage to the converter, (b) output voltage of the converter

In this research work, SPWM technique is used which is a carrier based PWM technique. In SPWM modulating signal is generated by comparing the pulses with the sine wave which helps in reducing distortion factor remarkably. The converter control is designed in Synchronous Reference Frame (SRF) with DC voltage control and AC current/voltage control using PI controller. The Phase Locked Loop (PLL) synchronizes the control by detecting the amplitude and the phase angle vector of the grid voltage/current [13]. The voltage at PCC can be expressed as;

$$V_{PCC-a} = \hat{V}\cos(\omega_0 t + \theta_0) \quad (12)$$

$$V_{PCC-a} = \hat{V}\cos\left(\omega_0 t + \theta_0 - \frac{2\pi}{3}\right) \quad (13)$$

$$V_{PCC-a} = \hat{V}\cos\left(\omega_0 t + \theta_0 + \frac{2\pi}{3}\right) \quad (14)$$

where $\hat{V}$ is the amplitude of PCC phase voltage in volts, $(\omega_0)$ is the system frequency in radian/sec and $(\theta_0)$ is initial phase-angle. The PCC voltage components in dq-frame are as:

$$V_{PCC-d} = \hat{V}\cos(\omega_0 t + \theta_0 - \varphi) \quad (15)$$

$$V_{PCC-q} = \hat{V}\sin(\omega_0 t + \theta_0 - \varphi) \quad (16)$$

Phase angle $\varphi$ should be so selected so as to avoid any time-variant function in dq components. Let us assume $\varphi = \varpi_0 t + \theta_0$ then $V_{PCC-d} = \hat{V}$ and $V_{PCC-q} = 0$. This results in dq components to be pure DC quantities. This is the fundamental mechanism of 3-Φ SRF-PLL. The designed inverter control is presented in Fig. 6. The source voltages are taken as reference signal which are the input to the PLL and abc-dq0 transformation. PI controller helps in obtaining error free output by rectifying the feedback error between a desired set-point input and the measured processed value. In case of SAM, a 3-Φ reference signal is considered to design the control.

| e-ISSN: 2278 – 8875, p-ISSN: 2320 – 3765| www.ijareeie.com | Impact Factor: 7.282|

|| Volume 10, Issue 12, December 2021 ||

DOI:10.15662/IJAREEIE.2021.1012029

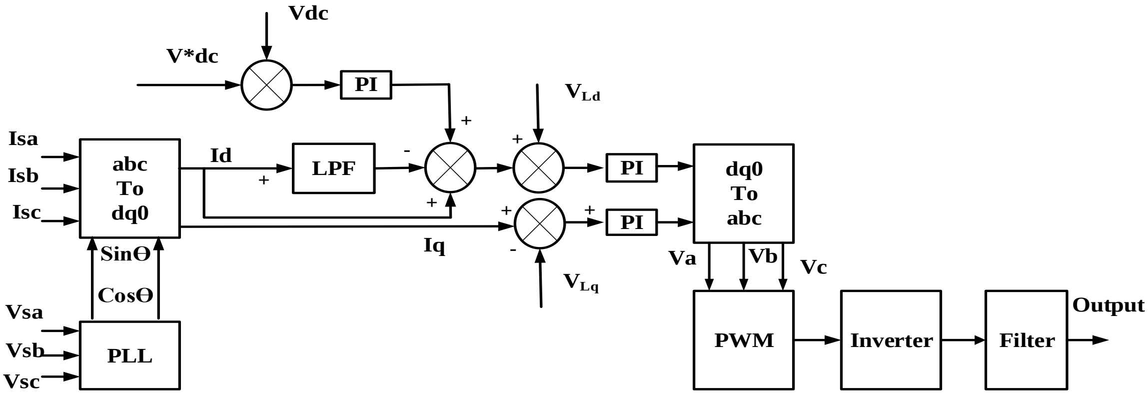


Fig. 5 Inverter control

## IV. SIMULATION RESULTS FOR SECS IN STAND-ALONE MODE (SAM)

In this research work a 15KW SECS is designed whose DC-output is 600 V as presented in Fig. 6. The parameter of the designed SECS is presented in Table 3. The system has been analyzing for both constant irradiance of 1000w/m$^2$and variation from 600 -1000w/m$^2$ from t = 1.5-3 sec. The output voltage and current for linear load of 10KW is presented in Fig. 7 and Fig.8 respectively. The power-flow is shown in Fig. 9 the load connected is linear therefore no reactive power is demanded. The system has been designed for 415V RMS for a peak value of 586V. For this system phase voltage will be 338.3 V as shown in Eq. 17.

$$V_{PH} = \frac{V_{L-L}}{\sqrt{3}} = \frac{586}{\sqrt{3}} = 338.2V \tag{17}$$

Where $V_{PH}$ is peak value of phase voltage and $V_{L-L}$ is peak value of line voltage.

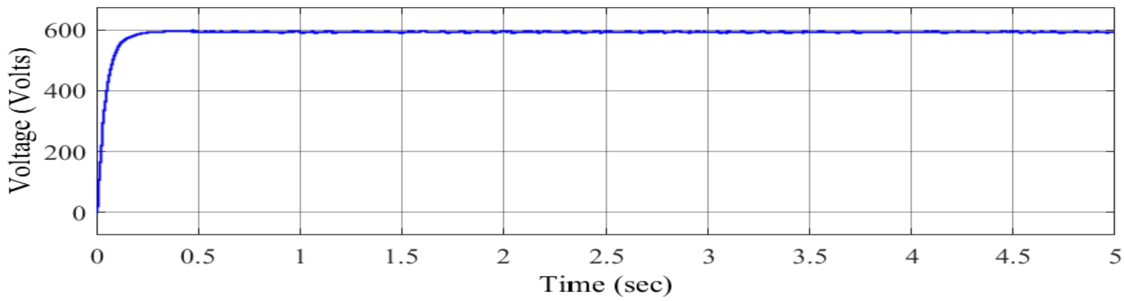


Fig. 6 Output DC voltage of boost converter for constant irradiance

Table 4. Parameters for the designed system

| PARAMETER | VALUE |
|---|---|
| RMS nominal Voltage | 415 V |
| Phase voltage | 338.2 V |
| Peak Voltage | 586 V |
| PV rating | 15KW |
| Filer resistance | 0.5Ω |
| Filter inductance | 10Mh |
| Filter conductance | 8.7Mf |
| Integral gain | 500 |
| Proportional gain | 0.04 |
| PWM switching ratio | 2000 |

| e-ISSN: 2278 – 8875, p-ISSN: 2320 – 3765| www.ijareeie.com | Impact Factor: 7.282|

|| Volume 10, Issue 12, December 2021 ||

DOI:10.15662/IJAREEIE.2021.1012029

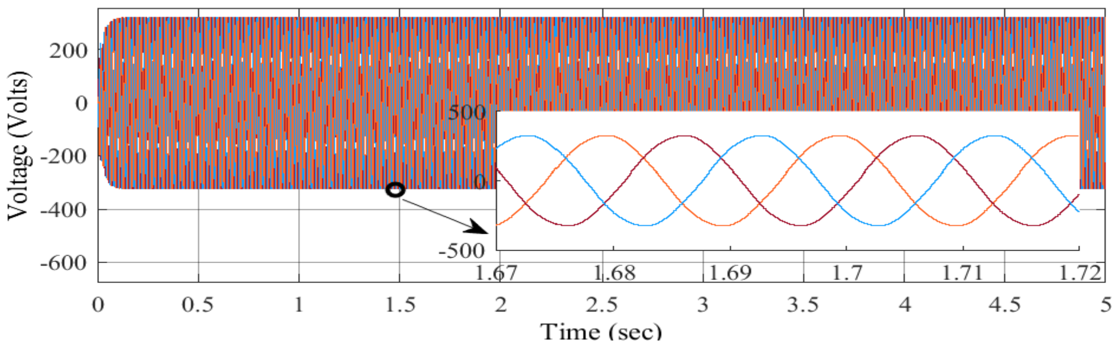


Fig. 7 Output voltage for constant irradiance in SAM

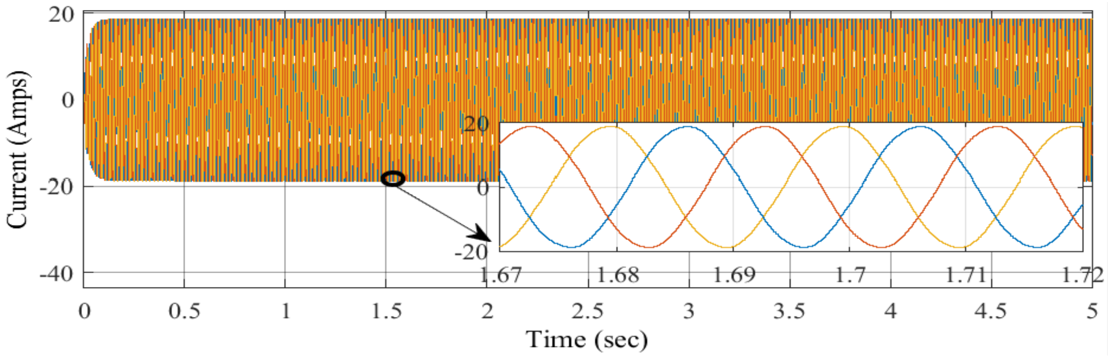


Fig. 8 Output current at load bus for constant irradiance in SAM

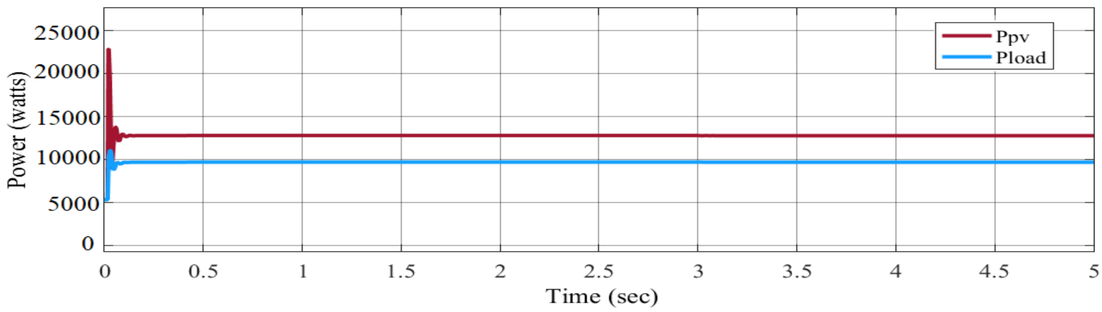


Fig. 9 Power-flow for constant irradiance in SAM

For analyzing system under variable irradiance, the solar irradiance is varied from 600 -1000 w/m2 for time t = 1.5-3 sec. The DC voltage for variable irradiance is shown in Fig. 10. The voltage and current are shown in Fig. 11 and Fig. 12 respectively.

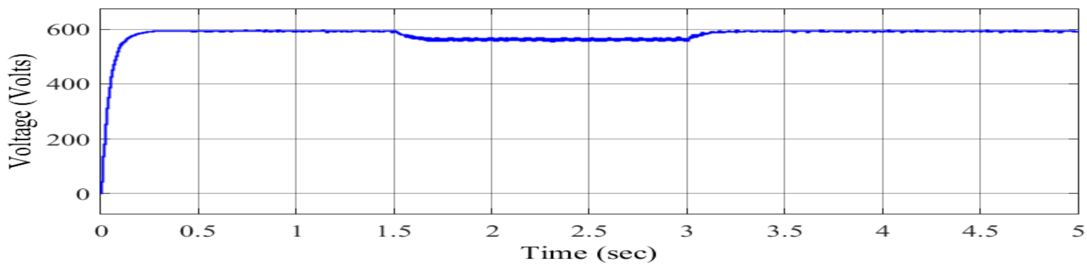


Fig. 10 DC voltage for variable irradiance

| e-ISSN: 2278 – 8875, p-ISSN: 2320 – 3765| www.ijareeie.com | Impact Factor: 7.282|

|| Volume 10, Issue 12, December 2021 ||

DOI:10.15662/IJAREEIE.2021.1012029

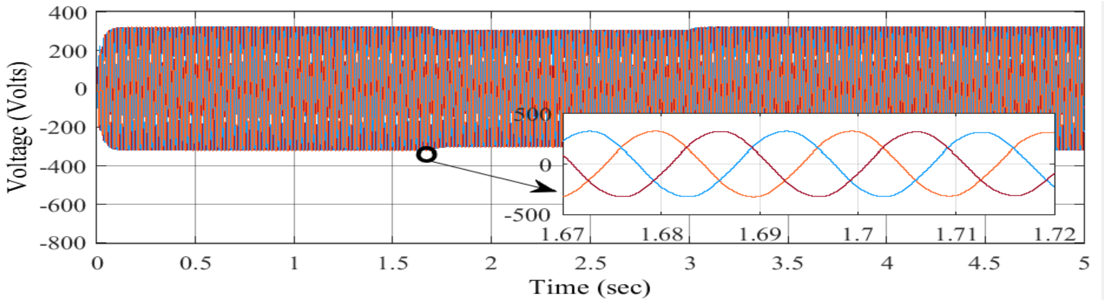


Fig. 11 Load-voltage for variable irradiance in SAM

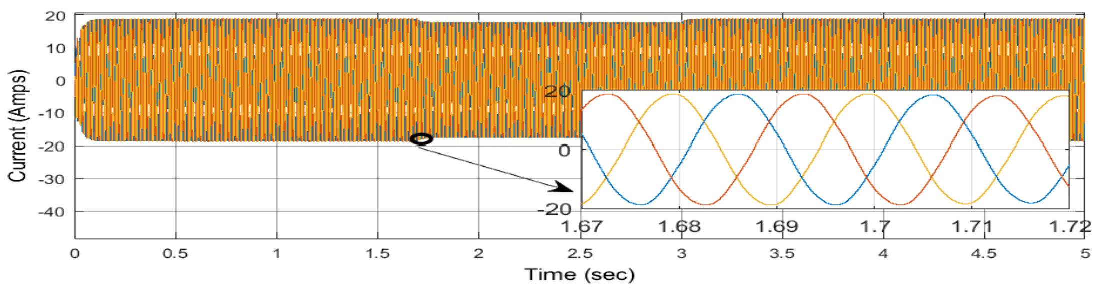


Fig. 12 Load-current for variable irradiance in SAM

From the voltage and current wave-shapes it can be seen that, though variation in irradiance also leads to the variation of voltage and current inverter side but it shows less variation as compared to the variation in irradiance. Irradiance is varied from 1000-600-1000 w/m$^2$ during t=1.5-3 sec and voltage varies from 335-280-335 V, while current varies from 19-15-19 A.

## V. OPERATION UNDER NON-LINEAR LOAD

A three-phase non-linear load having 40 Ω resistance connected across full-bridge rectifier is analyzing. Loads with non-linear behavior distort the system. The grid voltage and current at this condition is shown in Fig. 13 and Fig. 14 respectively. From the waveforms it can be observed that the non-linear distorts the grid voltage and current. The THD of the grid voltage (6.16%) and current (8.5%) is shown in Fig. 16. The load voltage is also distorted and contains the same harmonics as in grid voltage, while the load current harmonics are very high as shown in Fig. 17 and Fig. 18 respectively.

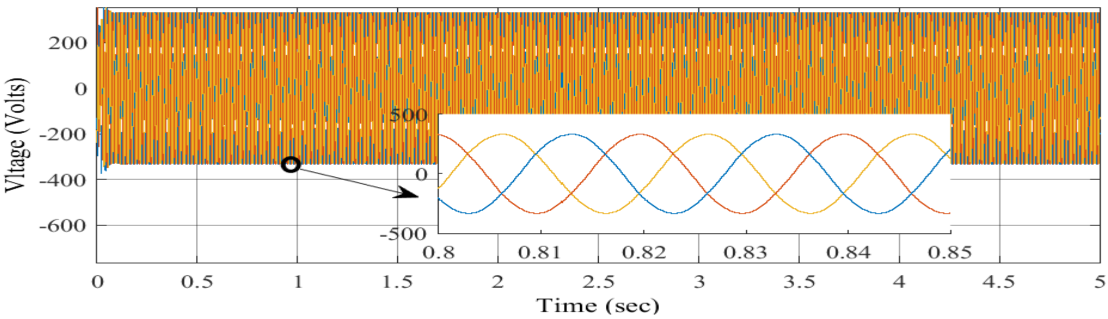


Fig. 13 Grid voltage for non-linear load

| e-ISSN: 2278 – 8875, p-ISSN: 2320 – 3765| www.ijareeie.com | Impact Factor: 7.282|

|| Volume 10, Issue 12, December 2021 ||

DOI:10.15662/IJAREEIE.2021.1012029

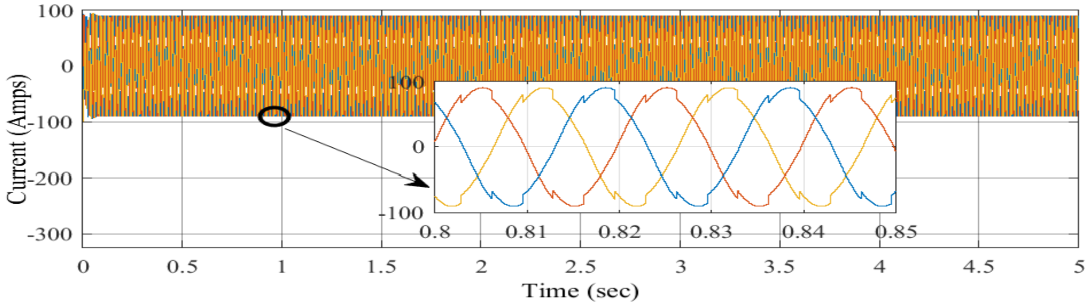


Fig. 14 Grid current for non-linear load

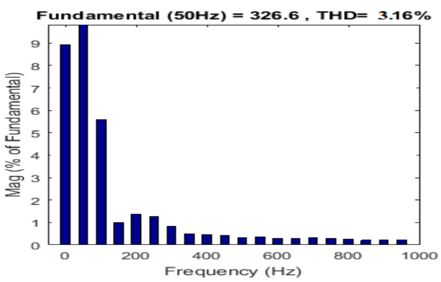


THD of voltages

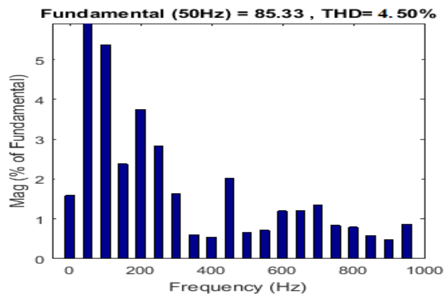


THD of currents

Fig.15 THD of PCC voltage and current with non-linear load

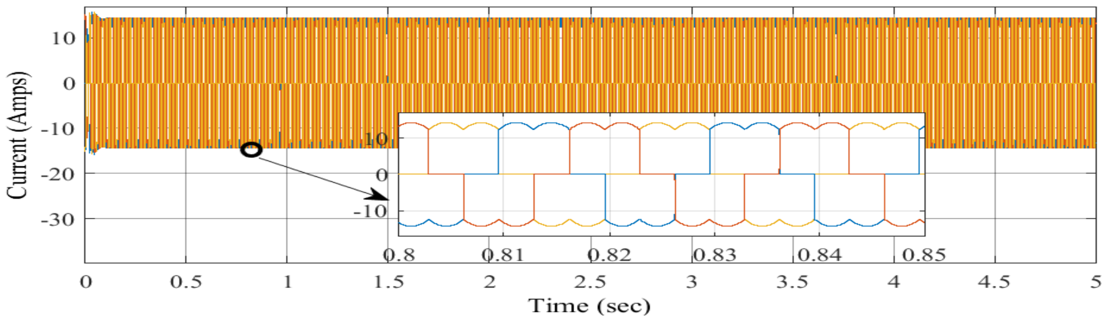


Fig. 16 Load current wave-shape for non-linear load

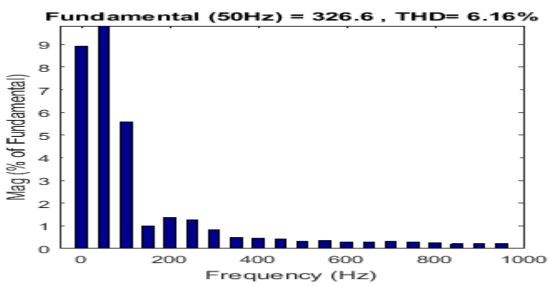


THD of voltages

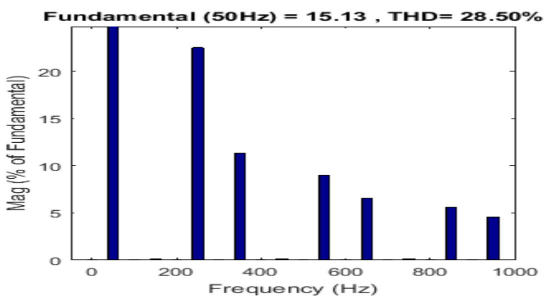


THD of currents

Fig.17 THD of load voltage and current with non-linear load

| e-ISSN: 2278 – 8875, p-ISSN: 2320 – 3765| www.ijareeie.com | Impact Factor: 7.282|

|| Volume 10, Issue 12, December 2021 ||

DOI:10.15662/IJAREEIE.2021.1012029

## VI. CONCLUSION

In this paper solar energy scenario in India is briefly described. The components of SECS is explained with mathematical modeling. The SECS is formed using PV-array whose DC output has been regulated using boost converter. The DC-AC converter converts the DC generated output of SECS into AC. The DC-AC converter is designed using two-level VSI whose control is designed using PQ-theory in SRF and PLL. The stand-alone operation of SECS is analyzing for rural electrification. The designed SECS is analyzing for reducing THD in PCC voltage and current since PEC injects harmonics and high harmonics content in voltage and current waveform may hinder the operation of sensitive load connected. SA-SECS is also analyzing for operating conditions like non-linear loading. It can be seen that the high THD adversely affects the performance of SECS leading to the generation of various PQ issues. The mitigation of these issues in SECS using proper controller for VSI is been presented in this paper.

## REFERENCES

[1]. M. G. Molina and L. E. Juanico, "Dynamic modelling and control design of advanced photovoltaic solar system for distributed generation applications," Journal of Electrical Engineering: Theory and Application, vol.1, No.3, pp. 141-150, January 2010.

[2]. Sachin Jain, and Vivek Agarwal, "A single-stage grid connected inverter topology for solar PV systems with maximum power point tracking", IEEE transactions on power electronics, vol. 22, no. 5, pp. 1928-1940, 2007.

[3]. Franco F. Yanine, Enzo E. Sauma, "Review of grid-tie micro-generation systems without energy storage, towards a new approach to sustainable hybrid energy systems linked to energy efficiency," Renewable and Sustainable Energy Reviews, vol. 26, pp. 60-95, October 2013.

[4]. K. H. Hussein, I. Muta, T. Hoshino, and M. Osakada, "Maximum photovoltaic power tracking: An algorithm for rapidly changing atmospheric conditions", Proc. Inst. Elect. Eng. Gener, Transmits. Distrib, vol. 142, no. 1, pp. 59–64, January 1995.

[5]. Reza Reisi, A Hassan Moradi M, Jamasb S., "Classification and comparison of maximum power point tracking techniques for photovoltaic system: A review", Renewable and Sustainable Energy Reviews, vol. 19, pp. 443-433 2013.

[6]. Hasaneen B M, Adel A. Elbaset Mohammed. Design and simulation of DC/DC boost converter. In Power System Conference, MEPCON 2008. 12th International Middle-East, IEEE 2008, pp. 335-340.

[7]. D Diallo, F Belkacem, Eric Berthelot. . Design and Control of a Low Power DC-DC Converter fed by a Photovoltaic array. IEEE International Conference on Electrical Machines and Drives IEMDC. pp. 1288-1293.

[8]. M Elshaer, A Mohamed, O Mohammed. Smart Optimal Control of DC-DC Boost Converter in PV Systems. IEEE/PES Conference Publication Transmission and Distribution Conference and Exposition, Nov 2010, pp. 403-410.

[9]. Hauke Brigitte. Basic calculation of a buck converter's power stage. Texas Instruments, Dallas, Texas, Tech. Rep. SLVA477 2014.

[10]. Hauke Brigitte. Basic calculation of a boost converter's power stage. Texas Instruments, Application Report. 2012

[11]. S. Alepuz, S. Busquets-Monge, J. Bordonau, J. Gago, D. Gonzalez, and J. Balcells, "Interfacing renewable energy source to the utility grid using a three-level inverter", IEEE Trans. Ind. Electron., vol. 53, no. 5, pp. 1504–1511, October 2006.

[12]. E. Pouresmaeil, D. Montesinos-Miracle, and O. Gomis-Bellmunt, "A multi objective control strategy for grid connection of distributed generation resources", Energy, vol. 35, no. 12, pp. 22–5030, December 2010.

[13]. Edris Pouresmaeil, Daniel Montesinos-Miracle, and Oriol Gomis-Bellmunt, "Control Scheme of Three-Level NPC Inverter for Integration of Renewable Energy Resources into AC Grid", IEEE Systems Journal, vol. 6, No. 2, June 2012.

[14]. Sandeep N., Prachi Salodkar, and P. S. Kulkarni. "A new simplified multilevel inverter topology for grid-connected application", IEEE Conference on Electrical, Electronics and Computer Science, pp. 1-5, 2014.

[15]. Jawairia Atiq, Prashant Kumar Soori, "Modelling of a Grid Connected Solar PV System Using MATLAB/Simulink", International Journal of Simulation: Systems, Science and Technology, vol. 17 No.41, pp. 45.1-45.7, March 2017.

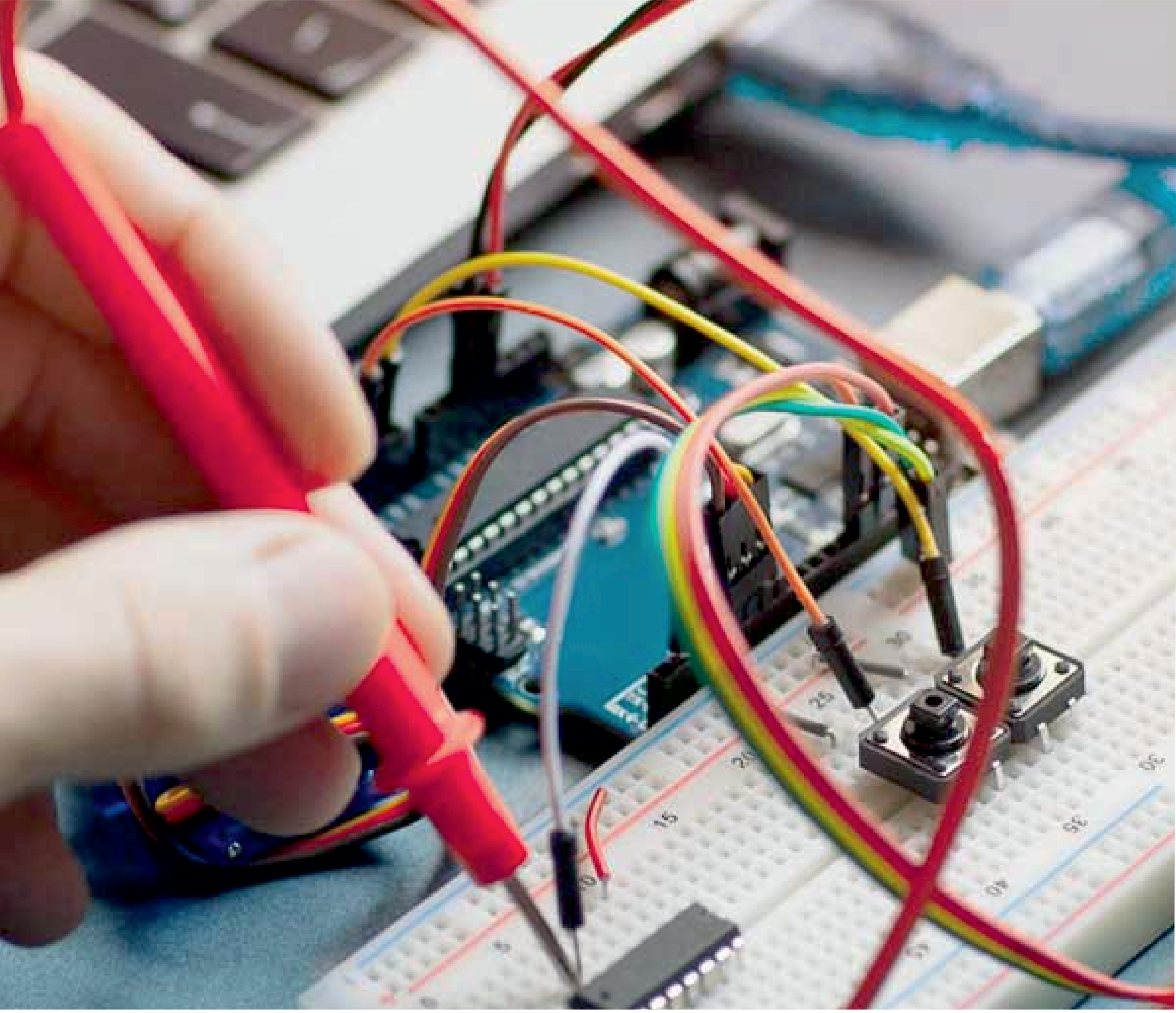


INNO SPACE

SJIF Scientific Journal Impact Factor

Impact Factor: 7.282

INTERNATIONAL STANDARD SERIAL NUMBER INDIA

निस्केयर NISCAIR


# International Journal of Advanced Research

## in Electrical, Electronics and Instrumentation Engineering


9940 572 462 6381 907 438 ijareeie@gmail.com